University of Massachusetts Dartmouth

Department of Mathematics

An Exploration of Statistical Methods in Determining the Gaussianity of LIGO Detector Data

A project in
Data Science
by
Ashish Thomas Mathew

Submitted in Partial Fulfillment of the
Requirements for the Degree of
Master of Science

May, 2025

Abstract

The Advanced Laser Interferometer Gravitational-wave Observatory (LIGO) is one of the most sophisticated instruments ever built, capable of measuring motion 10,000 times smaller than a proton, and was the first device to detect a Gravitational Wave (GW) event. Due to its high sensitivity, a common issue is its susceptibility to glitches: transient, non-Gaussian noise bursts occurring at a high enough rate to contaminate the time series data obtained from the detector. The current methods to detect and study glitches, though highly effective for analyzing the strain data during the detection run, prove to be slow when working with a large throughput of detector data. Here we study a few possible statistical approaches to detecting these glitches in the time-amplitude domain. By sampling the strain data, conditioning it, and employing tests of normality, mainly the Shapiro-Wilk test, the Kolmogorov-Smirnov test, and the Anderson-Darling test, we gauge their effectiveness in determining the Gaussianity of a sample time-series strain data from the detector. The alternate hypothesis of these tests, i.e., the sample belonging to a non-Gaussian distribution, indicates the presence of a glitch or a signal. The results of this experiment explore in detail the viability of these tests as efficient alternatives to the current solutions used in detecting a glitch or astrophysical event in a time series signal.

1 Introduction

Nearly a century after Einstein's prediction of the existence of Gravitational Waves (GWs) in 1916, the first direct gravitational wave detection was achieved by the Advanced Laser Interferometer Gravitational-Wave Observatory (aLIGO) and Virgo collaboration during the binary black hole merger event GW150914 on September 14, 2015. The LIGO Livingston (L1) interferometer underwent several upgrades following this run - effectively a massive redesign - enhancing its sensitivity by 15% to 25% [1]. This improvement was evident during the O2 observing run during which L1, in conjunction with its Hanford (H1) counterpart and Virgo (V1), detected eleven new gravitational wave signals [2]. Subsequently, during the O3 run, all three detectors operated at their best possible sensitivity, leading to the first single-detector GW detection, GW190425, achieved by LIGO Livingston [3]. There have been over 90 GW events recorded at a high level of confidence since the LIGO-Virgo collaboration's inception to date.

A consequence of these detectors' sensitivities is their susceptibility to noise. During observation runs, various noise sources, such as seismic noise, suspension thermal noise, and sensing noise, affect the data collected by the interferometers. All these sources collectively produce time series signals which can be treated as stochastic processes with their corresponding joint probability distributions and statistical properties [4]. In the absence of astronomical signals or glitches, the probability distribution of the noise follows a normal distribution, also known as *Gaussian* noise. In the event of a Gravitational wave or any other signal, the noise exhibits a high signal-to-noise ratio (SNR), making it *non-Gaussian*.

Among these noise sources, the most problematic are **glitches**: transient events caused by non-astrophysical phenomena such as anthropogenic noise, weather conditions, or instrument malfunctions [4, 5]. Glitches manifest as localized bursts of excess power in interferometer time series data and often do not have well-defined sources. They can occur at energy levels and frequencies that overlap with GW signals, thereby mimicking them and increasing the number of false positive detections. During the first half of the third observing run (O3a) LIGO Hanford and Livingston recorded glitches rates of 0.29 min^{-1} and 1.10 min^{-1} respectively, which rose to 0.32 min^{-1} and

1.17 min^{-1} during the second half (O3b) [6]. Of the 90 candidate events detected in this run, 17 had a probability of astronomical origin (p_{astro}) below 0.5, suggesting significant ambiguity about their origin. A notable example of glitches posing such an issue was during the binary neutron star merger event GW170817 [7], during which instrumental noise transients were detected before the event's coalescence time, complicating its detection and subsequent analysis.

Detecting and mitigating the effects of glitches in interferometric strain data remains an active area of research within astrophysical data analysis, with several techniques proposed and implemented for the same [8–10]. However, many of these are computationally expensive and lack the efficiency required for near-real-time assessment of the signals for glitch activity. The more popular solutions incorporate the *q-transform* [11, 12], a modification of the standard Fourier transform where the analysis window scales inversely with frequency. This q-transform computes a p-value depicting the statistical significance of excess power in the data. Assuming the background data to be Gaussian, the excess power that does not follow a Gaussian distribution suggests the presence of a glitch. While this method is effective for post-detection run analysis, it is ineffective for real-time use. Additionally, when scaled up to perform calculate on multiple samples, the computational time would increase significantly.

This project explores statistical hypothesis testing on time-amplitude domain data as a faster alternative to the current glitch detection methods working in the frequency domain. Building on the idea presented in [4], which treats detector noise as stochastic processes with joint probability distributions, it would be reasonable to assume that parametric and non-parametric statistical tests could be effectively applied to such data. This study focuses on applying (1) the Shapiro-Wilk test, (2) the Kolmogorov-Smirnov test, and (3) the Anderson-Darling test on preprocessed samples of clean and glitched data from the LIGO Livingston interferometer. The objective is to determine the normality of these samples and assess how well these tests differentiate between Gaussian (clean) and non-Gaussian (glitched) samples. This experiment also includes studying the distributions, waveforms, and frequency ranges, with particular emphasis on failure points for each statistical test across various glitch types. Furthermore, considering the frequency bands at which each glitch type occurs, this study also examines how each statistical test performs under band-pass filtering at various frequency ranges.

This report is organized as follows: Section 2 discusses how interferometer data is obtained and describes the properties of the time series data used in this study. It also outlines the process of acquiring clean and glitched samples and the preprocessing applied. Section 3 describes in detail the statistical tests of Gaussianity used to assess the sample data. The experimental procedures and results are presented in Sections 4 and 5. Finally, Section 6 summarizes the findings of our experiments, discussing the strengths and limitations of the methods, followed by the future scope in Section 7.

2 Data Acquisition and Conditioning

The Advanced LIGO and Virgo interferometers are large-scale, heavily modified versions of the Michelson interferometer (Figure 1a), originally invented by American physicist Albert A. Michelson in 1887 [6, 13]. LIGO operates in a vacuum, using a laser beam of light split into two orthogonal parts with the help of a half-silvered mirror mounted on horizontal seismometer suspensions. The orthogonally split beams are then sent through two arms of the interferometer, known as Fabry–Pérot cavities. Each of these arms is 4 kilometers long, consisting of mirrors at each end. The first of the mirrors is fixed in place, while the second one is movable with the help of precise micrometer drives. The laser beams, when reflected by the mirrors on either end of the arms, are combined again at the beam splitter and sent to photoelectric detectors. The aLIGO interferometer is designed such that if the beams travel equal distances, the recombination would lead to a destructive interference pattern, resulting in no light coming out of the instrument [14]. When a disturbance of either astrophysical or terrestrial origin is detected, an infinitesimally small change occurs in lengths of the detector arms, in the order of $10^{-8}m$ [15]. One of the arms is stretched, and the other arm is compressed in the perpendicular direction, altering the lengths of the reflected and combined beams, misaligning them and resulting in an interference pattern (Figure 1b). This interference pattern, coupled with results from several other sensors, provides detailed information on the *strain* of the GW or glitch event being observed.

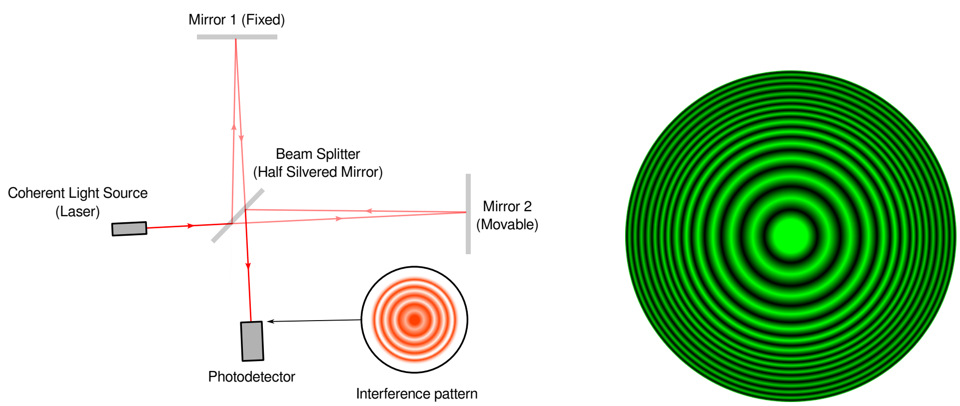

(a) Construction of an Interferometer

(b) Interference pattern

Figure 1: Illustrations of a basic Michelson interferometer [16, 17] and what an interference pattern would look like.

The `GWpy` Python package is widely used in this project. It provides a sute of tools to access and condition detector strain data from the Gravitational-Wave Open Science Centre (GWOSC) database [18]. This data is in the time domain, as timestamps in the GPS time system at nanosecond precision, and records the amplitude of the noise event as a differential change in lengths of the interferometer arms. GWpy handles detector data using the `TimeSeries` object, which is built upon `numpy` arrays. This allows compatibility with most of the core numpy utilities along with custom functions for signal processing, tabular data filtering, and visualization.

We use the strain data from LIGO Livingston (L1) during the first part of the third observing run (O3a) for this project due to the high rate of occurrence of glitches. Figure 2 shows the steps taken to acquire signal data from the detector and condition it for statistical testing.

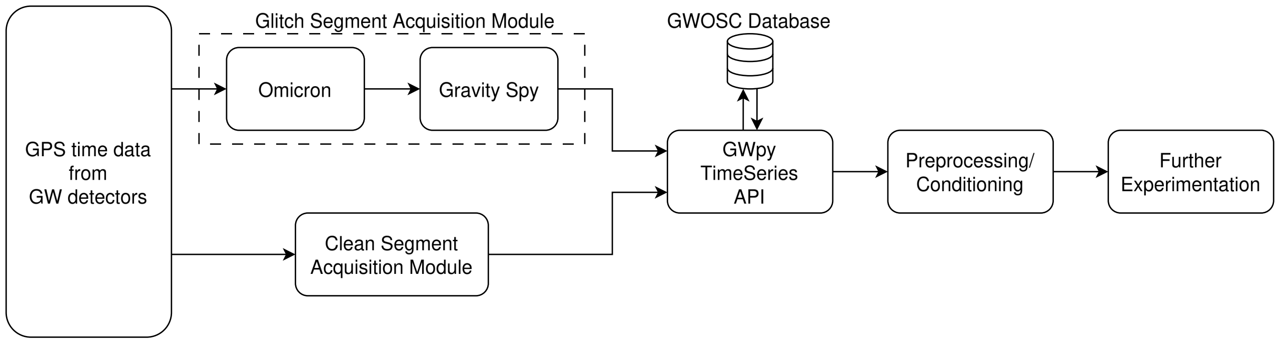

Figure 2: The Data Acquisition and Conditioning Pipeline

There are two main types of detector samples that we receive from the detectors: **Glitched detector data** and **Clean detector data**. The following sections will go a bit deeper into each of these types of data and how they are obtained.

2.1 Glitch data

The GPS times of glitch occurrences are obtained using *Gravity Spy* [19], a large-scale citizen-science project that combines astrophysics, machine learning, and human efforts to classify glitches in GW interferometer data. The *Omicron* transient search algorithm is used by Gravity Spy to generate q-transform spectrograms and calculate SNR of the time series samples [8]. This algorithm is crucial in identifying the most useful samples for data classification and analysis. Based on the morphological characteristics from the spectrograms, a total of 22 glitch classes were identified with an SNR above 7.5 and peak frequencies between 10 Hz and 2048 Hz.

In the O3a data for L1, Fast_Scattering and Tomte glitches are the most prevalent, while Chirp, 1080Lines and Wandering_line glitches have fewer samples, as shown in Table 1. The No_Glitch class represents glitch samples that lack significant traits or energy levels and do not fit in with the other classes morphologically. Hence, for our study, we do not consider this glitch class.

Glitch Class	Count	Glitch Class	Count
Fast_Scattering	21749	Whistle	896
Tomte	18708	Low_Frequency_Lines	788
Blip_Low_Frequency	7549	Scratchy	207
Scattered_Light	5398	Repeating_Blips	164
No_Glitch	5358	Violin_Mode	164
Extremely_Loud	4319	Paired_Doves	155
Koi_Fish	4268	Light_Modulation	72
1400Ripples	2363	Helix	21
Blip	1947	Wandering_Line	20
Power_Line	1189	1080Lines	9
Low_Frequency_Burst	1187	Chirp	6

Table 1: Glitch counts per class for LIGO Livingston (L1) during the O3a run.

Using the glitch GPS times, the time series information is obtained from the GWOSC database using the `TimeSeries.fetch_open_data()` API provided by GWpy. Here, a time window of 10 seconds is taken on either side of each of the GPS times with the glitch in the center, sampled at a rate of 4096 Hz. The TimeSeries objects obtained are then conditioned for statistical testing and cropped down to a 1-second time window around the glitch for further use.

2.2 Clean Samples

The process of finding gaps of clean detector noise is done using `gwtrigfind`, a package developed to search for event triggers files from GW detectors, in conjunction with `EventTable`, provided by GWpy.

Taking the start and end GPS times of the O3a run, gwtrigfind is used to find the file path containing Omicron triggers from the *L1:GDS-CALIB_STRAIN* channel of the L1 detector. EventTable is then used to load all the trigger data, containing information on the start and end GPS times of the events. Taking the time frames between the end and start times of successive events, we obtain the gaps between glitches/GW triggers, which do not have a significant amount of noise activity. The sizes of the gaps are clamped between 7 and 30 seconds because too short of a gap could lead to the inclusion of glitches in the sample, as the time series data may not have enough time to stabilize after a glitch; and too long of a time gap could be indicative of detector malfunction or a period of time when it is not operational.

The GPS start and end times of the clean segments are then used to calculate their Q-transform and corresponding p-values. The GPS time intervals with a p-value greater than 0.95 are considered to be clean segments of data, and are used to obtain the corresponding TimeSeries data from GWpy. The TimeSeries data is then, similar to the glitch data, conditioned for statistical testing and cropped down to 1-second samples for further use.

2.3 Data Conditioning

The strain readings obtained from a GW detector are usually a combination of the GW signal and detector noise. In most cases, the noise in the GW detectors is stationary [5], i.e. the characteristics of the noise do not change over time, hence keeping the statistical properties constant. However, this is not the case with glitches. Glitches, as discussed in the introduction (1) are transient, non-Stationary, non-Gaussian events caused by various environmental factors. These can occur at any time during the observation run and can have a significant impact on the data collected by the detectors. Despite their sources being unknown, they have a large variety of time-frequency morphologies that help characterize them better. During detection runs, glitches show up as short-lived spikes of power in the time series data, increasing the noise floor and affecting the estimation of the power spectral density (PSD) of the data.

2.3.1 Power Spectral Density and Amplitude Spectral Density

The **Power Spectral Density (PSD)** is a method to represent how power is distributed across different frequencies in a signal [20, 21]. It is calculated by taking the average of the square of the Fast Fourier transforms (FFT) of the time series data, decomposing the signal into its constituent frequencies. The PSD provides a measure of how much power or strain noise is present at each frequency, allowing for the identification of dominant frequency components and their corresponding amplitudes.

One way to visualize the timeseries data is by using its **Amplitude Spectral Density (ASD)** values, which are found by taking the square root of the PSD.

$$ASD(f) = \sqrt{PSD(f)} \tag{1}$$

ASD measures the amplitude of the signal at each frequency, and it is often used to compare the noise levels of different detectors or to assess a detector's sensitivity to specific frequencies. The ASD is normally plotted on a logarithmic scale, with frequency on the x-axis and the ASD on the y-axis, allowing for easy identification of noise peaks and their corresponding frequencies.

Figure 3 shows an example of the ASD plot of a Tomte glitch event. To obtain the root-mean-square strain noise at a given frequency band, we integrate over the squares of the ASD readings over the frequency band of interest and take its square root. Observing the strong spectral lines at around the 300, 512, and 1024 Hz ranges, marked by dotted lines, there is a big chance that these are of instrumental origin. The problem with this plot, however, is that it does not capture the glitch signal well because glitches are relatively weak, highly transient and easily overpowered by the instrument noise. To better visualize the glitch, we would need to **whiten** the data and view its time-amplitude plot.

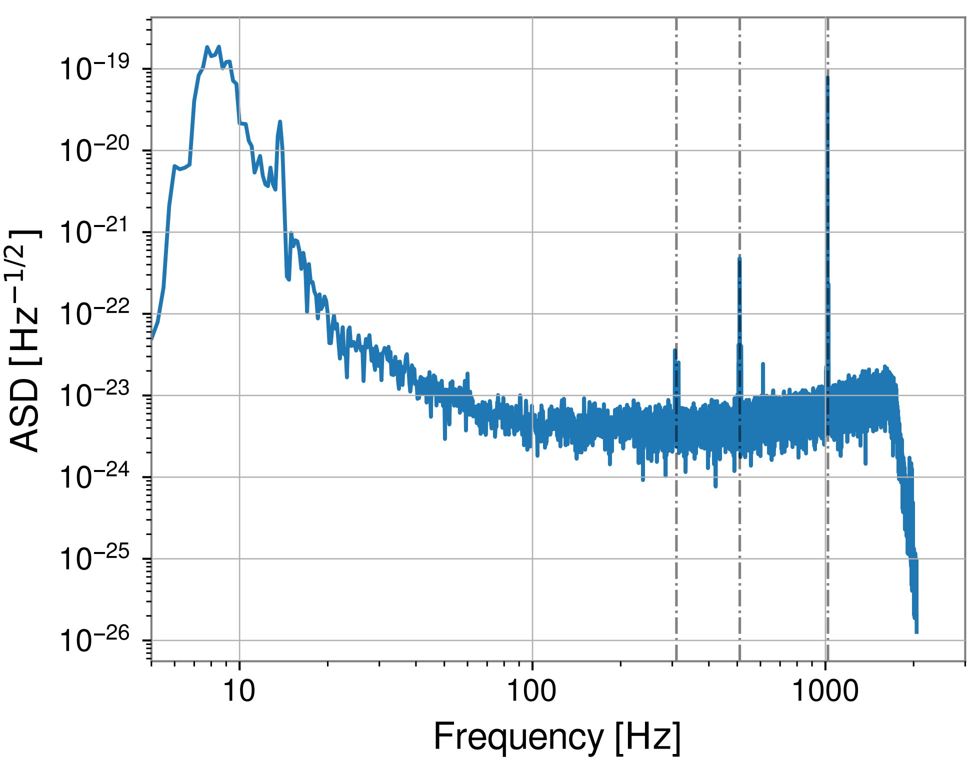

Figure 3: ASD plot for a Tomte Glitch.

2.3.2 Whitening

Whitening is the process of supressing low-frequency and spectral line noise from the data to allow for a clearer view of the weaker signals at sensitive frequency ranges. Whitening is one of the first steps in astrophysical data analysis, especially when the noise is highly non-stationary and can vary significantly over time. By whitening the data, we effectively reduce the impact of noise on our analysis, improving the sensitivity of our detection methods.

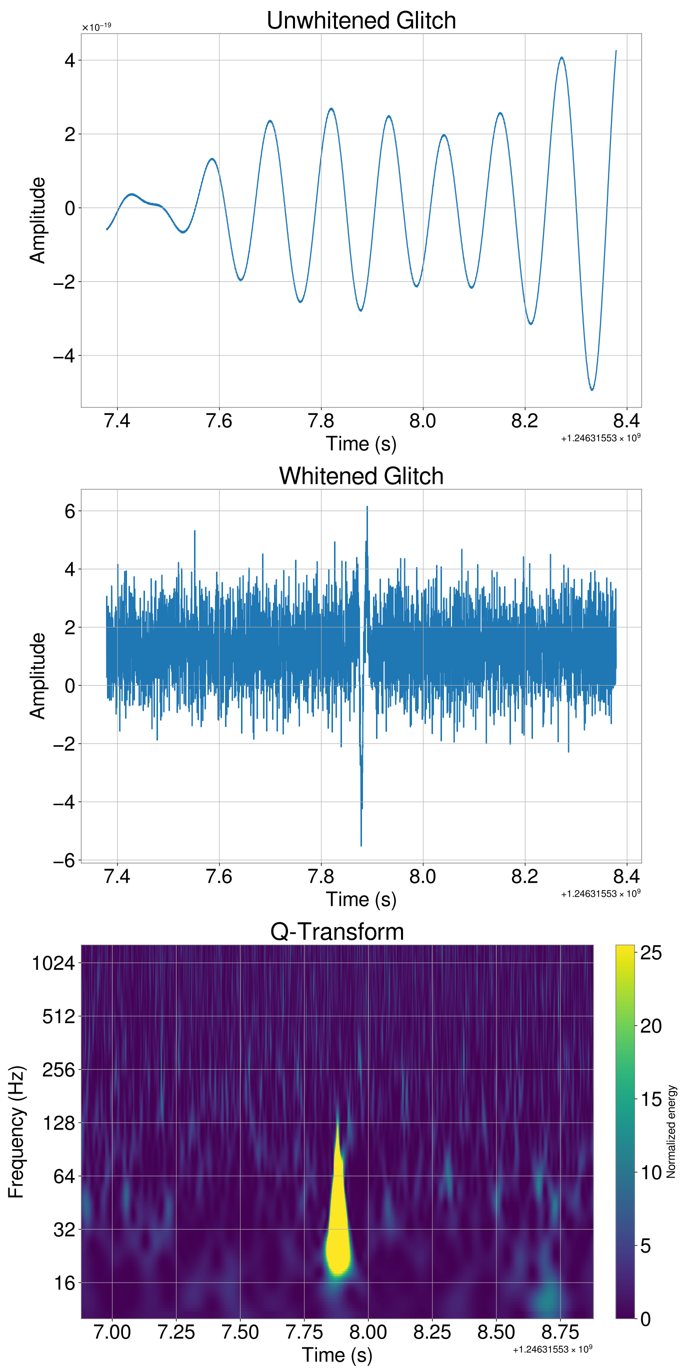

Figure 4: Example of a Tomte glitch signal before and after whitening.

Figure 4 shows a Tomte glitch signal before and after whitening. In the first plot we do not clearly

see the effects of the glitch on the timeseries data. As we can see, the whitening process has effectively flattened the noise floor, allowing for a clearer view of the glitch signal.
This is done by taking the inverse of the ASD and multiplying it with the original time series data. This effectively flattens the noise floor, allowing for a clearer view of the glitch signal. The resulting whitened data can then be used for further analysis, such as statistical testing or machine learning classification.

2.3.3 Filtering

3 Methods

3.1 Motivation

3.2 Shapiro-Wilks Test

3.3 KS

3.4 AD

4 Experimentation with the complete frequency range

5 Experimentation with a band pass filter applied

6 Conclusions

7 Future Scope

8 Appendix

References

[1] Andrew Grant. “Advanced LIGO ramps up, with slight improvements”. en. In: *Physics Today* 2016.11 (Nov. 2016), p. 12128. ISSN: 19450699. DOI: 10.1063/pt.5.9074. URL: https://pubs.aip.org/physicstoday/online/12128 (visited on 04/05/2025).

[2] The LIGO Scientific Collaboration, the Virgo Collaboration, et al. “GWTC-1: A Gravitational-Wave Transient Catalog of Compact Binary Mergers Observed by LIGO and Virgo during the First and Second Observing Runs”. In: *Physical Review X* 9.3 (Sept. 2019). arXiv:1811.12907 [astro-ph], p. 031040. ISSN: 2160-3308. DOI: 10.1103/PhysRevX.9.031040. URL: http://arxiv.org/abs/1811.12907 (visited on 04/05/2025).

[3] R. Abbott et al. *GWTC-2: Compact Binary Coalescences Observed by LIGO and Virgo During the First Half of the Third Observing Run*. arXiv:2010.14527 [gr-qc]. Mar. 2021. DOI: 10.1103/PhysRevX.11.021053. URL: http://arxiv.org/abs/2010.14527.

[4] The LIGO Scientific Collaboration, the Virgo Collaboration, et al. "A guide to LIGO-Virgo detector noise and extraction of transient gravitational-wave signals". In: *Classical and Quantum Gravity* 37.5 (Mar. 2020). arXiv:1908.11170 [gr-qc], p. 055002. ISSN: 0264-9381, 1361-6382. DOI: 10.1088/1361-6382/ab685e. URL: http://arxiv.org/abs/1908.11170 (visited on 04/12/2025).

[5] The LIGO Scientific Collaboration and the Virgo Collaboration. "Characterization of transient noise in Advanced LIGO relevant to gravitational wave signal GW150914". In: *Classical and Quantum Gravity* 33.13 (July 2016). arXiv:1602.03844 [gr-qc], p. 134001. ISSN: 0264-9381, 1361-6382. DOI: 10.1088/0264-9381/33/13/134001. URL: http://arxiv.org/abs/1602.03844 (visited on 04/11/2025).

[6] The LIGO Scientific Collaboration, the Virgo Collaboration, et al. *GWTC-3: Compact Binary Coalescences Observed by LIGO and Virgo During the Second Part of the Third Observing Run*. arXiv:2111.03606 [gr-qc]. Oct. 2023. DOI: 10.1103/PhysRevX.13.041039. URL: http://arxiv.org/abs/2111.03606.

[7] The LIGO Scientific Collaboration and The Virgo Collaboration. "GW170817: Observation of Gravitational Waves from a Binary Neutron Star Inspiral". In: *Physical Review Letters* 119.16 (Oct. 2017). arXiv:1710.05832 [gr-qc], p. 161101. ISSN: 0031-9007, 1079-7114. DOI: 10.1103/PhysRevLett.119.161101. URL: http://arxiv.org/abs/1710.05832 (visited on 04/17/2025).

[8] Florent Robinet et al. "Omicron: A tool to characterize transient noise in gravitational-wave detectors". In: *SoftwareX* 12 (2020), p. 100620. ISSN: 2352-7110. DOI: https://doi.org/10.1016/j.softx.2020.100620. URL: https://www.sciencedirect.com/science/article/pii/S2352711020303332.

[9] Duncan M. Macleod et al. "GWpy: A Python package for gravitational-wave astrophysics". In: *SoftwareX* 13 (2021), p. 100657. ISSN: 2352-7110. DOI: https://doi.org/10.1016/j.softx.2021.100657. URL: https://www.sciencedirect.com/science/article/pii/S2352711021000029.

[10] D. Davis et al. "Subtracting glitches from gravitational-wave detector data during the third observing run". In: *Classical and Quantum Gravity* 39.24 (Dec. 2022). arXiv:2207.03429 [astro-ph], p. 245013. ISSN: 0264-9381, 1361-6382. DOI: 10.1088/1361-6382/aca238. URL: http://arxiv.org/abs/2207.03429.

[11] S. Chatterji et al. "Multiresolution techniques for the detection of gravitational-wave bursts". In: *Classical and Quantum Gravity* 21.20 (Oct. 2004). arXiv:gr-qc/0412119, S1809–S1818. ISSN: 0264-9381, 1361-6382. DOI: 10.1088/0264-9381/21/20/024. URL: http://arxiv.org/abs/gr-qc/0412119 (visited on 04/15/2025).

[12] Leah Vazsonyi and Derek Davis. "Identifying glitches near gravitational-wave signals from compact binary coalescences using the Q-transform". In: *Classical and Quantum Gravity* 40.3 (Feb. 2023). arXiv:2208.12338 [astro-ph], p. 035008. ISSN: 0264-9381, 1361-6382. DOI: 10.1088/1361-6382/acafd2. URL: http://arxiv.org/abs/2208.12338 (visited on 04/14/2025).

[13] R. Weiss et al. *Quarterly Progress Report No. 105*. Apr. 1972. URL: https://dspace.mit.edu/handle/1721.1/56271.

[14] The LIGO Scientific Collaboration. *What is an Interferometer?* URL: https://www.ligo.caltech.edu/page/what-is-interferometer (visited on 04/07/2025).

[15] Sudarshan Ghonge et al. *Assessing and Mitigating the Impact of Glitches on Gravitational-Wave Parameter Estimation: a Model Agnostic Approach*. arXiv:2311.09159 [gr-qc]. Oct. 2024. DOI: 10.48550/arXiv.2311.09159. URL: http://arxiv.org/abs/2311.09159.

[16] Stannered. *Simple Michelson interferometer diagram*. 2007. URL: https://commons.wikimedia.org/wiki/File:Interferometer.svg.

[17] WiredSense. *The Michelson Interferometer - A Laser Lab Alignment Guide*. WiredSense Tutorials. URL: https://www.wiredsense.com/tutorial/the-michelson-interferometer-a-laser-lab-alignment-guide.

[18] D. M. Macleod et al. "GWpy: A Python package for gravitational-wave astrophysics". In: *SoftwareX* 13 (2021), p. 100657. ISSN: 2352-7110. DOI: 10.1016/j.softx.2021.100657. URL: https://www.sciencedirect.com/science/article/pii/S2352711021000029.

[19] M Zevin et al. "Gravity Spy: integrating advanced LIGO detector characterization, machine learning, and citizen science". In: *Classical and Quantum Gravity* 34.6 (Feb. 2017), p. 064003. ISSN: 1361-6382. DOI: 10.1088/1361-6382/aa5cea. URL: http://dx.doi.org/10.1088/1361-6382/aa5cea.

[20] Alan V. Oppenheim and Ronald W. Schafer. *Discrete-Time Signal Processing*. 3rd. USA: Prentice Hall Press, 2009. ISBN: 0131988425.

[21] M. Lopez. "Exploring the Frontier of Transient Gravitational Wave Detection - Unleashing the Power of Machine Learning". PhD thesis. Utrecht University, 2025.